Estimating Satellite and Receiver Differential Code Bias Using Relative GPS Network

Alaa A. Elghazouly[1], Mohamed I. Doma[1], Ahmed A. Sedeek[2]

[1] Faculty of Engineering, Menoufia University, Egypt.

[2] EL Behira Higher Institute of Engineering and Technology, El Behira, Egypt.

Correspondence: Alaa A. Elghazouly (alaa_elghazouly@sh-eng.menofia.edu.eg)

Abstract

Precise Total Electron Content (TEC) are required to produce accurate spatial and temporal resolution of Global Ionosphere Maps (GIMs). Receivers and Satellites Differential Code Biases (DCBs) are one of the main error sources in estimating precise TEC from Global Positioning Systems (GPS) data. Recently, researchers are interested in developing models and algorithms to compute DCBs of receivers and satellites close to those computed from the Ionosphere Associated Analysis Centers (IAAC). Here we introduce a MATLAB code called Multi Station DCB Estimation (MSDCBE) to calculate satellites and receivers DCBs from GPS data. MSDCBE based on spherical harmonic function and geometry free combination of GPS carrier phase and pseudo-range code observations and weighted least square were applied to solve observation equations, to improve estimation of DCBs values. There are many factors affecting estimated value of DCBs. The first one is the observations weighting function which depending on the satellite elevation angle. The second factor concerned with estimating DCBs using single GPS Station used by Zero Difference DCB Estimation (ZDDCBE) code or using GPS network used by MSDCBE code. The third factor is the number of GPS receivers in the network. Results from MSDCBE were evaluated and compared with data from IAAC and other codes like M_DCB and ZDDCBE. The results of weighted (MSDCBE) least square shows an improvement for estimated DCBs, where mean differences from Center for Orbit Determination in Europe (CODE) (University of Bern, Switzerland) less than 0.746 ns. DCBs estimated from GPS network shows a good agreement with IAAC than DCBs estimated from PPP where the mean differences are less than 0.1477 ns and 1.1866 ns, respectively. The mean differences of computed DCBs improved by increasing number of GPS stations in the network.

Keywords: DCBs, Multi station, elevation angle, number of stations.

1. Introduction

TEC is an important parameter in the study of ionospheric dynamics, structures, and variabilities. The ionosphere is a dispersive medium for space geodetic techniques operating in the microwave band (Böhm, and Schuh, 2013) that allows calculation of TEC using GPS dual-frequency radio transmissions. The global availability of GPS has made it a valuable tool for sensing the Earth' the regional and global ionosphere estimation (Hernández-Pajares et al. 1999; Komjathy et al. 2005; Li et al. 2015; Liu and Gao 2004; Mannucci et al. 1993). Unfortunately, GPS-derived TEC measurements are adversely affected by an inherent interfrequency bias within the receiver and satellite hardware, typically referred to as the DCBs. Careful estimation of the DCBs is required to obtain accurate TEC, which is used in several applications, such as in several ionospheric prediction models, and in the correction of GPS positioning measurements (McCaffrey et al., 2017). A number of methods have been proposed for the estimation of GPS receiver DCBs, each with varying requirements and limitations including making assumptions about the ionospheric structure; the use of internal calibration (Arikan et al., 2008; Themens et al., 2013,2015); or the use of a reference instrument or model. Estimating DCBs for receivers and satellites from GPS observations depending on two approaches, the relative and absolute methods. The relative method utilizes a GPS network, while the absolute method determines DCBs from a single station (Sedeek et al., 2017). In the current study, we applied relative method to calculate DCBs of satellites and GPS receivers.

There has also been growing interest in measuring the accuracy of these methods, and how different factors, e.g. ionospheric activity, plays a role in these methods (McCaffrey et al., 2017). Nowadays, reliable GIMs and accurate DCBs of satellites and The International GNSS Service (IGS) stations can be obtained from IAAC like CODE (Schaer,1999), European Space Agency (ESA, Germany) (Feltens and Schaer, 1998), Jet Propulsion Laboratory (JPL, USA) (Mannucci et al., 1998), and UPC (Technical University of Catalonia, Spain) (Hernández-Pajaresetal.,1999; Orús et al.,2005). However, the availability of IAAC DCB receivers' values, it is only available for IGS stations. Furthermore, some of IGS ground receiver DCB estimates are not available from all analysis centers. Also, some regions don't have any IGS ground stations like our country Egypt, which mean the TEC values over them would be interpolated from nearest calculated values. As TEC values depended on DCB values it is required a mathematical model to calculate DCBs from GPS data.

In this study we introduce a mathematical model estimating satellites & receiver DCBs for a GPS network based on Spherical Harmonic Function (SHF) written under MATLAB environment, the developed mathematical model uses geometry free combination of pseudo-range observables (P-code). Weighted Least Square was used to consider variation of satellites elevation angle. The code was evaluated and compared with other researchers' codes in section "Results and analysis". In the "Conclusion" section we summarize the overall paper results.

2. GPS Observation Model

For a GPS satellite, the pseudorange and carrier phase observations between a receiver and a satellite can be expressed as (Jin et al., 2008; Leandro, 2009; Leick et al., 2015; Zhang et al., 2018):

$$P_{r,j}^s(i) = \rho_r^s(i) + c(dt_r - dt^s) + T_r^s + I_{r,j,P}^s + DCB_r^P - DCB_s^P + M_j + E_j \qquad (1)$$

59 $$\Phi_{r,j}^s(i) = \rho_r^s(i) + c(dt_r - dt^s) + T_r^s - I_{r,j,\Phi}^s + \lambda_j N_j + pb_{r,j} - pb_{s,j} + DCB_r^\Phi - DCB_s^\Phi + m_j + e_j \qquad (2)$$

60 With r, s, j and i the receiver, satellite, frequency and epoch indices, and where:

61   $P_{r,j}^s(i)$ Pseudo-range measurements, in meter,

62   $\Phi_{r,j}^s(i)$ carrier-phase measurements, in meter,

63   $\rho_r^s(i)$ the geometric distance between satellite and receiver antennas, in meters,

64   c   the speed of light, in meters per second,

65   dt_r and dt^s receiver and satellite clock errors, respectively, in seconds,

66   T_r^s the neutral troposphere delay, in meters,

67   $I_{r,j,P}^s$ and $I_{r,j,\Phi}^s$ the ionosphere delay of pseudo range and carrier phase observations, in meters,

68   N_j carrier-phase integer ambiguities, in cycles,

69   λ_j carrier-phase wave length, in meters,

70   $DCB_{r,}^p$ and DCB_s^p receiver and satellite pseudo-range hardware delays, respectively in metric units,

71   DCB_r^Φ and DCB_s^Φ receiver and satellite carrier-phase hardware delays, respectively, in metric units,

72   Mj   Pseudo-range multipath on, in meters,

73   Ej   Other un-modeled errors of pseudo-range measurements, in meters,

74   pbr,i and pbs,i   receiver and satellite carrier-phase initial phase bias, respectively, in metric units,

75   mj   carrier-phase multipath, in meters and

76   ej   Other un-modeled errors of carrier-phase measurements, in meters.

77 Here, we consider a measurement scenario that one GPS receiver tracks dual frequency code and phase data from a total of m
78 satellites over t epochs, thereby implying r = 1, s = 1, ….. m, j = 1, 2 and i = 1, ….., t.

79 Firstly, the code read the Rinex files and extract the pseudo range and carrier phase observations which are the range distances
80 between the receivers and satellites measured using L_1 and L_2 frequencies. The "geometry-free" linear combination of GPS
81 observations is used to derive the observable. The geometric range, clock-offsets and tropospheric delay are frequency
82 independent and can be eliminated using this combination. The "geometry-free" linear combinations for pseudo range and
83 carrier phase observations are given as (Al-Fanek 2013):

84 $$P_4 = P_{r,1}^s(i) - P_{r,2}^s(i) = I_{r,1,p}^S - I_{r,2,p}^S + DCB_r^p + DCB_s^p + E_{12} \qquad (3)$$

85 $$\Phi_4 = \Phi_{r,1}^s(i) - \Phi_{r,2}^s(i) = I_{r,2,\Phi}^S - I_{r,1,\Phi}^S + \lambda_1 N_1 - \lambda_2 N_2 + DCB_r^\Phi + DCB_s^\Phi + e_{12} \qquad (4)$$

86 $E_{12} = \sqrt{(E_1)^2 + (E_2)^2}$ is the combination of multipath and measurement noise on $P_{r,1}^s(i)$ and $P_{r,2}^s(i)$ (m), and

87 $e_{12} = \sqrt{(e_1)^2 + (e_2)^2}$ is the combination of multipath and measurement noise on $\Phi_{r,1}^s(i)$ and $\Phi_{r,2}^s(i)$ (m).

88 To reduce the multipath and noise level in the pseudo range observables, the carrier phase measurements are used to compute
89 a more precise relative smoothed range. Although the carrier-phase observables are more precise than the code derived, they
90 are ambiguous due to the presence of integer phase ambiguities in the carrier phase measurements. To take advantage of the
91 low-noise carrier phase derived and unambiguous nature of the pseudo range, both measurements are combined to collect the
92 best of both observations.

93 Smoothed $P_{4,sm}$ observations can be expressed as follows (Jin et al. 2012):

94 $$P_{4,sm} = \omega_t P_4(t) + (1 - \omega_t)P_{4,prd}(t) \qquad (t > 1) \qquad (5)$$

95 where t stands for the epoch number, ω_t is the weight factor related with epoch t, and

96 $$P_{4,prd}(t) = P_{4,sm}(t-1) + [L_4(t) - L_4(t-1)] \qquad (t > 1) \qquad (6)$$

97 when t is equal to 1, which means the first epoch of one observation arc, $P_{4,sm}$ is equal to P_4.

98

99 **3. Spherical Harmonic Model**

100 To determine the receiver DCB, there are two different methods. The first one is to calibrate the receiver device and obtain the
101 DCB directly. This method calculates the DCB of the receiver device ignoring that from the antenna cabling used during
102 observation (Hansen, 2002). The second method calculates the receiver DCB as a part of GPS signal time delay which is
103 independent on type of antenna. MSDCBE code works as the second methods (figure1).

104 The ionosphere delay can be expressed as follows (Abid et al. 2016):

105 $$d_{ion} = \frac{40.3}{f^2} STEC \qquad (7)$$

106 Where f stands for the frequency of the carrier and Slant Total Electron Content (STEC) is the total electron content along the
107 path of the signal. The observation equation can be formed by Substituting (7) into (3), and replacing P_4 by
108 smoothed $P_{4,sm}$, we get (Abid et al. 2016):

109 $$P_{4,sm} = 40.3\left(\frac{1}{f_1^2} - \frac{1}{f_2^2}\right)STEC + c * DCB_r + c * DCB_s \qquad (8)$$

110 Where: c is the speed of light and DCB_r and DCB_s are differential code bias for receiver and satellites in seconds.

STEC can be translated into Vertical Total Electron Content (VTEC) using the modified single-layer model (MSLM) (Haines 1985, Jin et al. 2012):

$$VTEC = MF(z)STEC \tag{9}$$

$$MF = \cos\left(arcsin\left(\frac{R}{R+H}sin(\alpha z)\right)\right) \tag{10}$$

Where:

MF   is the mapping function,

z   is the satellite elevation angle,

R   is the radius of the Earth=6371 km and

H   is the attitude of the ionosphere thin shell (assumed as used by CODE=506.7 km), α=0.9782 (Jin et al. 2012).

To estimate the satellite and receiver HDs, the current study applies a model based on spherical harmonic function to calculate them using zero-difference observations. The used model is expressed as follows (Schaer 1999, Li et al. 2015, Elghazouly et al, 2019):

$$VTEC(\beta,s)= \sum_{n=0}^{N}\sum_{m=0}^{n} P_n^m(sin(\beta))(A_n^m cos(m\lambda) + B_n^m sin(m\lambda)) \tag{11}$$

Where:

β is the geocentric latitude of IPPs (Ionosphere Peirce Point),

s   is the solar fixed longitude of IPPs,

N   is the degree of the spherical function,

M   is the order of spherical harmonic function; fourth order is used.

P_{mn} is regularization Legendre series and

A_{mn} and B_{mn} are the estimated spherical harmonics coefficients.

By substituting eq (8), eq (10) and eq (11) into eq (9) we get:

$$\sum_{n=0}^{N}\sum_{m=0}^{n} P_n^m(sin(\beta))(A_n^m cos(m\lambda) + B_n^m sin(m\lambda))$$

$$= \cos\left(arcsin\left(\frac{R}{R+H}sin(\alpha z)\right)\right)\left[-\frac{f_1^2 f_2^2}{40.3(f_1^2 - f_2^2)}(P_{4,sm} - c*DCB_r - c*DCB_s)\right] \tag{12}$$

Only one GPS station has more than 20,000 observations per a day. When applying equation (12) using stations observation data, there are number of equations much more than the number of unknown coefficients. These coefficients were determined using weighted least square method. general form of weighted least square function can be expressed as (Ghilani and Wolf, 2012):

$$X=(A^T PA)^{-1}A^T PL \tag{13}$$

Where:

X   is the unknown parameters vector namely, $A_n^m, B_n^m, DCB_r \ and \ DCB_s$,

A   is the coefficient (design) matrix (coefficients of $A_n^m, B_n^m, DCB_r \ and \ DCB_s$),

L   is the observation vector (values of $P_{4,sm}$) and

P   is the weight matrix.

As known, the quality of observations is affected by satellite elevation angle, each observation has a weight value depend on its satellite elevation angle. The weight value can be computed from the following equations (14, 15 and 16) (Luo X., 2013):

$$w = \frac{\sigma_0^2}{\sigma^2} \tag{14}$$

$$\sigma^2 = \left[0.05 + \frac{0.02}{sin(z)^2}\right]^2 \tag{15}$$

$$\sigma_0^2 = (f + d)^2 \tag{16}$$

Where:

f & d   are two constants equal to 5 and 2 cm, respectively (Ray and Griffiths 2008).
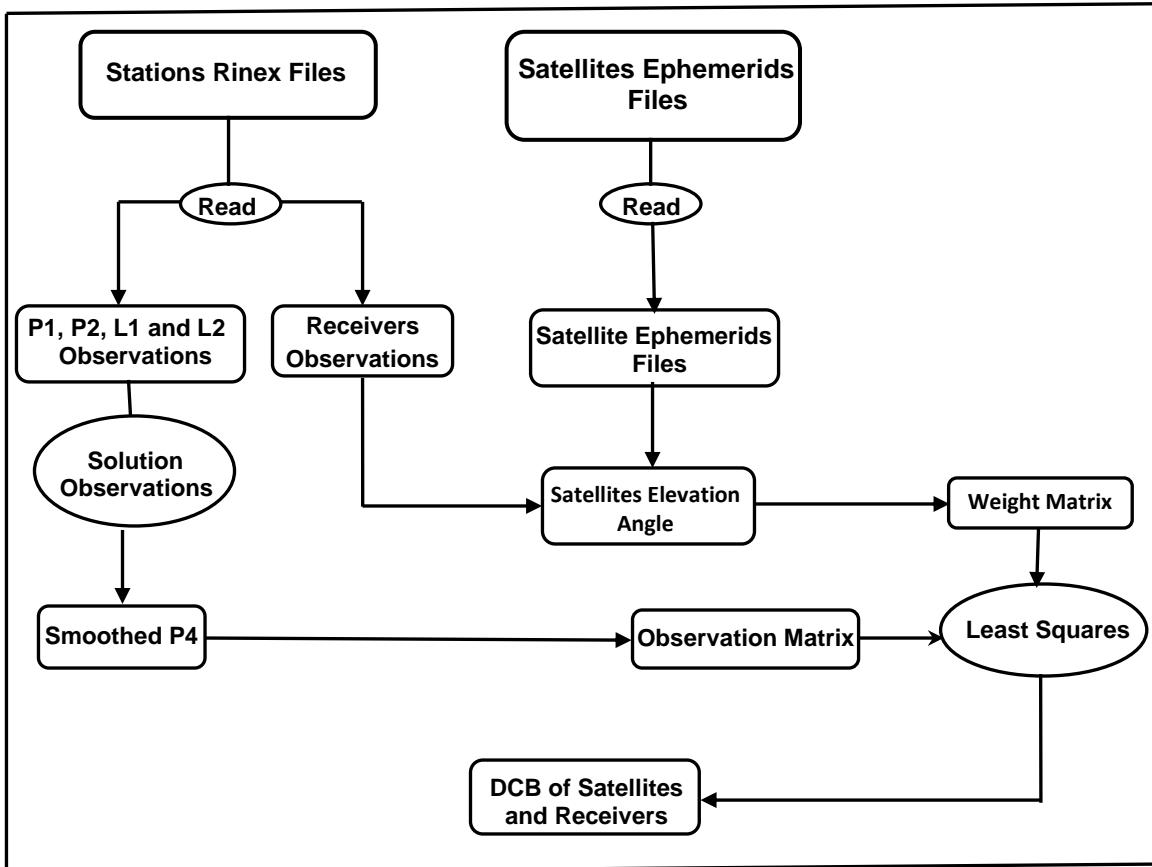
151 **Figure 1** Flow chart shows how the code works

1. Mathematical Model Evaluation

The MSDCBE software was written in MATLAB (version 2016a). The first input is GPS observations in Receiver Independent Exchange (RINEX) format according to the selected stations (figure 2) downloaded from (ftp://garner.ucsd.edu/rinex) and precise ephemerides (SP3) files of test days downloaded from (http://www.GPScalendar.com/index.html?year=2010). In addition, IONosphere Map EXchange Format (IONEX) files of IGS, CODE and JPL are downloaded - as a threshold values - from (ftp://cddis.gsfc.nasa.gov/GPS/products/ionex/).

In the present contribution, to evaluate the performance of the developed model, numerical case-studies were performed. The main goals of the numerical case-studies are to investigate three issues:

First issue is to investigate the effect of applying weighted least square instead of least square on satellites and GPS receiver DCBs, and this is done by comparing results from MSDCBE which applying weighted least square with the published results of M_DCB by Jin et al. (2012), and with those of IAAC.

BOGO, BRUS, GOPE, GRAS, ONSA, POTS, PTBB, SOFI and WTZA IGS Stations data from 1 to 31 January 2010 were applied as it was the same network used by Jin et al. (2012).

Second issue is to investigate the correlation between size (number of receivers) of the GPS network and estimated DCBs for satellite and GPS receiver, and this is done by comparing DCB values of three stations namely, GOPE, GRAS and ONSA estimated from a network consists of 3 GPS receiver and a network consists of 9 GPS receiver.

This study was applied using IGS Stations data from 1 to 5 January 2010 of six stations namely, BOGO, BRUS, GOPE, GRAS, ONSA, POTS, PTBB, SOFI and WTZA.

Third issue is to investigate the congruence of DCBs estimated from absolute and relative methods with other IAAC, and this is done by comparing results from MSDCBE with the published results of ZDDCBE by Sedeek et al. (2017).

This study was applied using data from 1 to 5 January 2010 of six stations namely, GOPE, GRAS, ONSA, MADR, PTBB, and SOFI which was the same network used by Jin et al. (2012) and Sedeek et al. (2017).
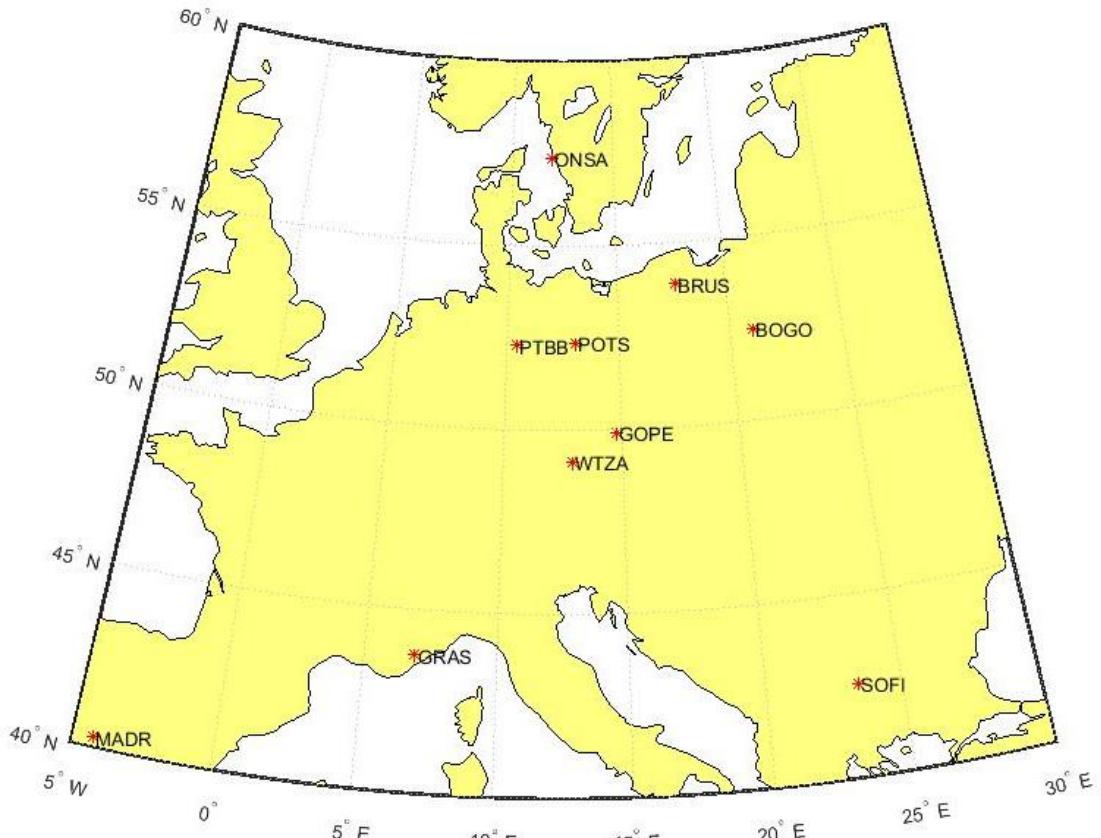
175
176 **Figure 2** IGS Stations locations

Comparison of multi-station test results from MSDCBE and M_DCB

178 The first evaluation made by this paper is the evaluation of weight function. MSDCBE used a weight function depending on
179 the satellite elevation angle as mentioned before. Table 1 shows the differences and RMS between satellites and receivers
180 estimated from 1 to 31 January 2010 using multiple GPS stations of both MSDCBE (weighted) and M_DCB (unweighted).

181 **Table 1** the differences and RMS between satellites and receivers estimated from 1 to 31 January 2010 using multiple GPS
182 stations (MSDCBE and M_DCB minus CODE).

satellite	MSDCBE		M_DCB		satellite	MSDCBE		M_DCB	
	differences(ns)	RMS	differences(ns)	RMS		differences(ns)	RMS	differences(ns)	RMS
G1	0.228	0.250	0.746	0.251	G17	0.087	0.125	0.038	0.138
G2	0.121	0.091	-0.073	0.087	G18	-0.136	0.113	-0.044	0.100
G3	0.004	0.078	0.194	0.066	G19	0.236	0.095	0.381	0.066
G4	0.169	0.092	0.003	0.123	G20	0.096	0.096	0.004	0.073
G5	-0.082	0.106	-0.236	0.111	G21	-0.208	0.109	-0.121	0.088
G6	-0.059	0.066	0.169	0.061	G22	-0.188	0.091	0.050	0.109
G7	-0.015	0.084	-0.233	0.085	G23	0.210	0.082	0.052	0.053
G8	-0.094	0.085	-0.271	0.085	G24	-0.168	0.086	-0.221	0.076
G9	0.011	0.074	0.038	0.088	G25	-0.091	0.122	-0.220	0.085
G10	-0.068	0.088	-0.343	0.095	G26	-0.302	0.089	-0.020	0.092
G11	0.211	0.090	0.202	0.063	G27	0.078	0.062	0.060	0.088
G12	0.029	0.059	0.049	0.051	G28	-0.177	0.080	-0.340	0.107
G13	0.296	0.080	0.140	0.062	G29	-0.195	0.128	-0.277	0.091
G14	-0.058	0.124	0.150	0.126	G30	0.057	0.077	0.020	0.074
G15	-0.055	0.101	-0.164	0.117	G31	0.018	0.099	0.057	0.138
G16	-0.057	0.069	0.096	0.084	G32	0.102	0.070	0.115	0.077
BOGO	0.139	0.077	0.065	0.080	POTS	0.120	0.073	0.237	0.094
BRUS	0.121	0.120	0.309	0.111	PTBB	0.083	0.082	0.201	0.095
GOPE	0.150	0.069	0.142	0.068	SOFI	-0.045	0.119	0.081	0.113
GRAS	0.085	0.125	0.370	0.131	WTZA	0.137	0.078	0.270	0.083
ONSA	0.140	0.093	0.178	0.103					

183 From the table one can see that the differences of MSDCBE estimated satellites DCBs are less than 0.302 ns and the RMS of
184 all satellites DCBs differences are less than 0.128 except G1 whose RMS = 0.250. The maximum difference of MSDCBE
185 estimated receivers DCBs is 0.150 ns of receiver GOPE and the minimum is 0.045 ns of receiver SOFI (Figure 3). The
186 maximum RMS of MSDCBE estimated receivers DCBs is 0.125. On the other side, M_DCB results show that Receiver DCB

biases are slightly larger than those for satellites, but most of them are less than 0.4 ns except G1 whose DCB bias reaches 0.746 ns. The RMS of all differences is lower than 0.3 ns (Jin et al. 2012). Figure 4 shows the mean differences between receiver DCB values estimated by MSDCBE and those released by CODE, IGS, and JPL combined from 1-31 Jan 2010. The figure shows that the results of MSDCBE are mostly close to those of CODE than IGS and JPL. By comparing the figure 4 with the corresponding chart published by Jin et al. (2012), it is clearly appeared that all differences between MSDCBE receivers' DCBs results and between CODE, IGS and JPL are less than those from M_DCB except station GOPE almost equal.
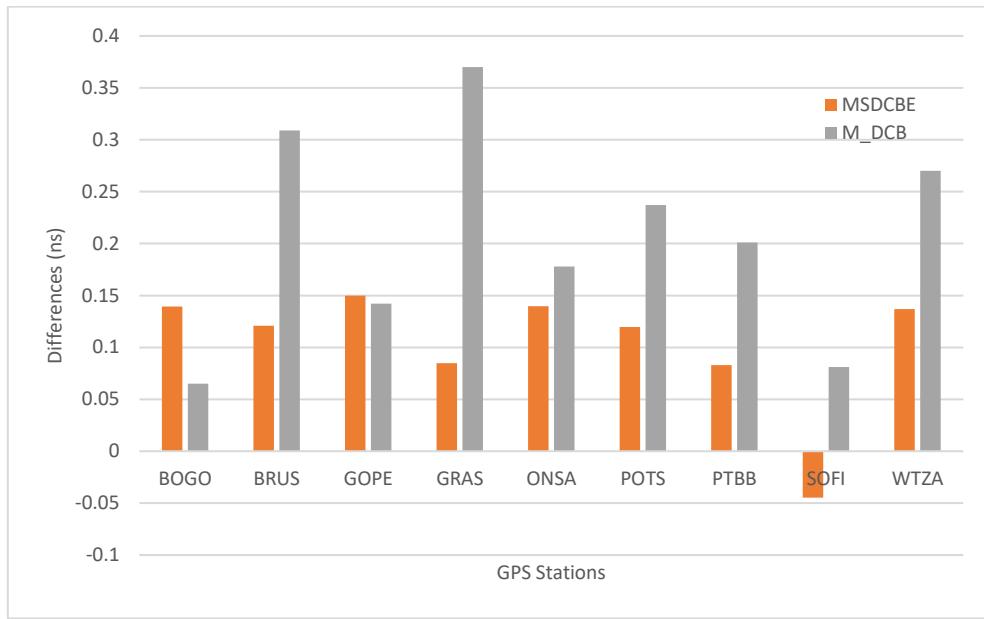
Figure 3 Mean difference between the receiver DCB values of CODE and the computed values by each of MSDCBE and M_DCB estimated from (1-31) Jan 2010.
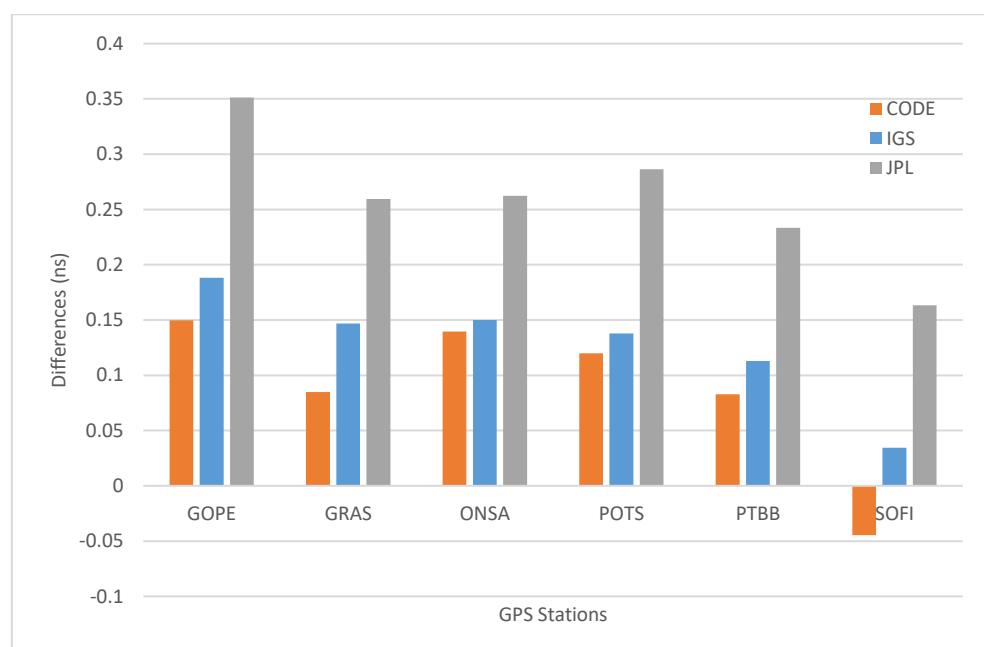
Figure 4 Mean differences between receiver DCB values estimated by MSDCBE and those released by CODE, JPL, and IGS combined from 1-31 Jan 2010.

Effect of network size factor on DCB estimation

By using multi station DCBs estimation, the number of stations used will appear as a factor influences DCBs estimation. This test was done by comparing DCBs computed by MSDCBE of a network of three receivers namely GOPE, GRAS, ONSA and DCBs of the same receivers but this time as a part of a network of nine receivers namely BOGO, BRUS, GOPE, GRAS, ONSA, PTBB, SOFI and WTZA. Figure 5 shows these results which demonstrate that using nine receivers gives more accurate DCBs. Also, the satellites DCBs differences (figure 6) almost improved but not like receivers DCBs, because satellites DCBs are small values compared with those of receivers.
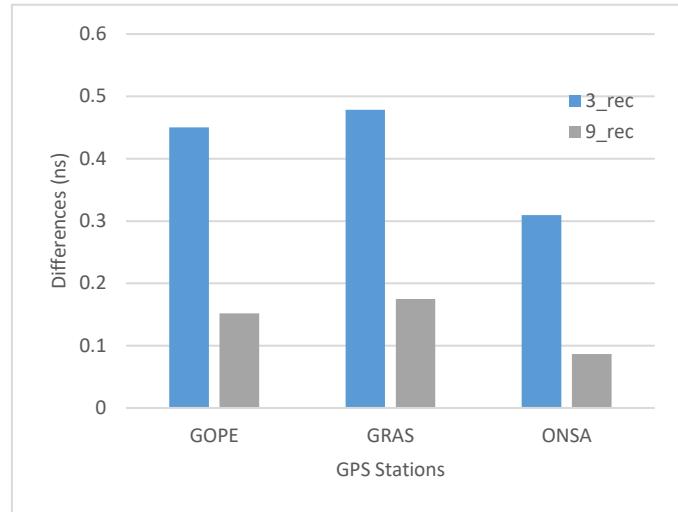
Figure 5 Mean difference between the receiver DCB values of IGS and the computed values by MSDCBE estimated from (1-5) Jan 2010.
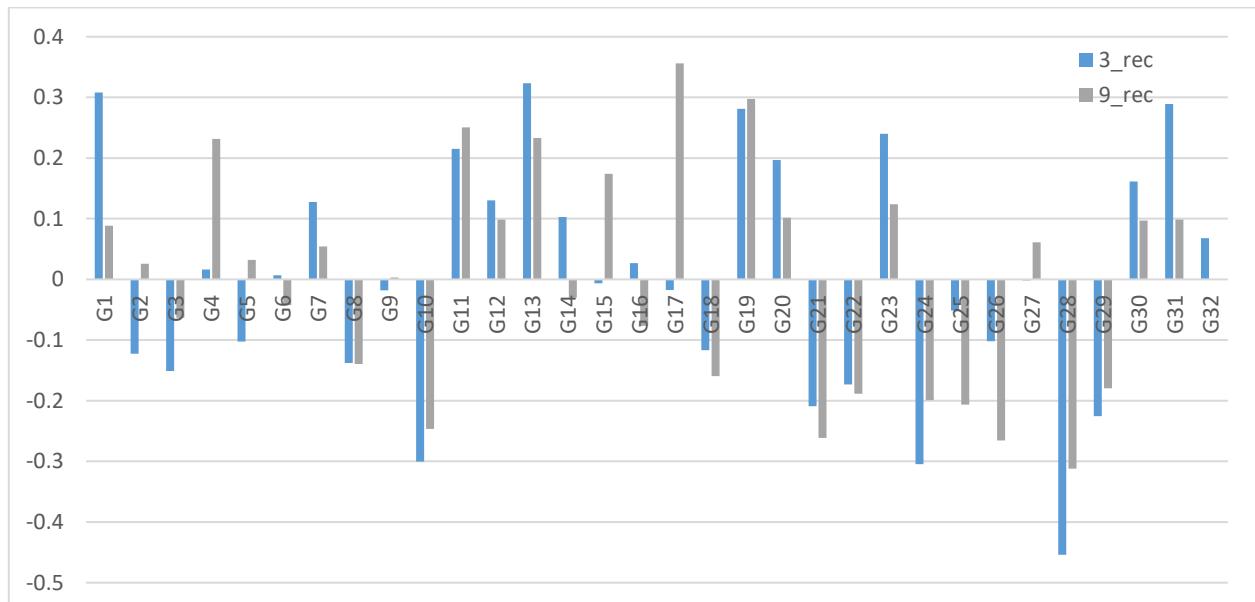
Figure 6 Mean difference between the satellites DCB values of IGS and the computed values by MSDCBE estimated from (1-5) Jan 2010

Comparison of multi-station from MSDCBE and single station from ZDDCBE and M_DCB test results

In this section the performance of multi station network against single station DCB estimation will be evaluated. Table 2 shows the mean deference between the receiver DCB values computed by IGS and the computed values by each of M_DCB, ZDDCBE and MSDCBE estimated from 1-5 Jan 2010. Figure 7 shows these results graphically and figure 8 shows the mean differences computed from M_DCB, ZDDCBE and MSDCBE for GPS satellites. The results show a significant difference between multi station network against single station DCB estimation. The maximum difference between receiver DCB estimation using IGS and MSDCBE is 0.1477 ns of MADR station, but it is 1.1866 ns and 0.7982 ns for M_DCB and ZDDCBE respectively.

Table 2 Mean deference between the receiver DCB values computed by IGS and the computed values by using single station M_DCB, ZDDCBE and multi-station MSDCBE estimated from 1-5 Jan 2010.

IGS St.	Model	DCB diff. (ns)	IGS St.	Model	DCB diff. (ns)
GOPE	M_DCB	0.3847	**ONSA**	M_DCB	1.1866
	ZDDCBE	0.1724		ZDDCBE	0.7982
	MSDCBE	0.004		MSDCBE	-0.0310
GRAS	M_DCB	0.3379	**PTBB**	M_DCB	0.6692
	ZDDCBE	0.1466		ZDDCBE	0.3550
	MSDCBE	0.066		MSDCBE	-0.0578
MADR	M_DCB	0.3078	**SOFI**	M_DCB	0.6916
	ZDDCBE	0.3468		ZDDCBE	0.4650
	MSDCBE	0.1477		MSDCBE	-0.0149
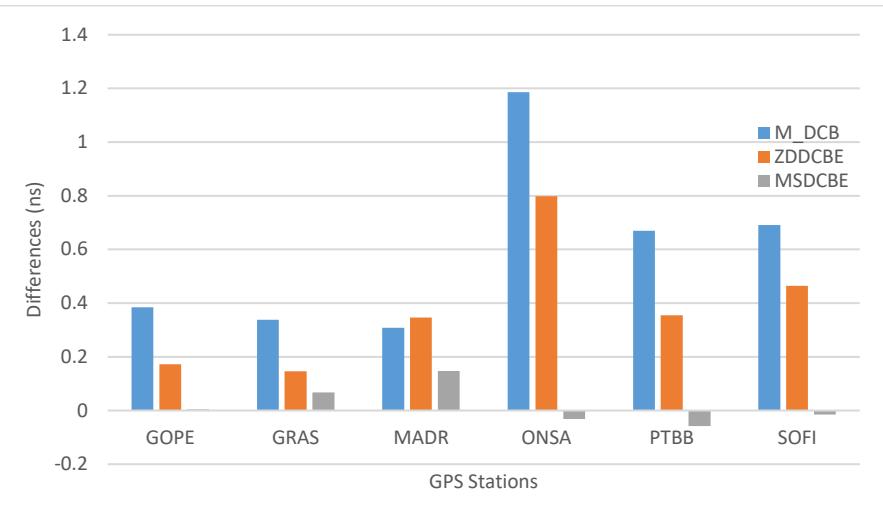
Figure 7 Mean difference between the receiver DCB values of IGS and the computed values by each of M_DCB, ZDDCBE and MSDCBE estimated from (1-5) Jan 2010
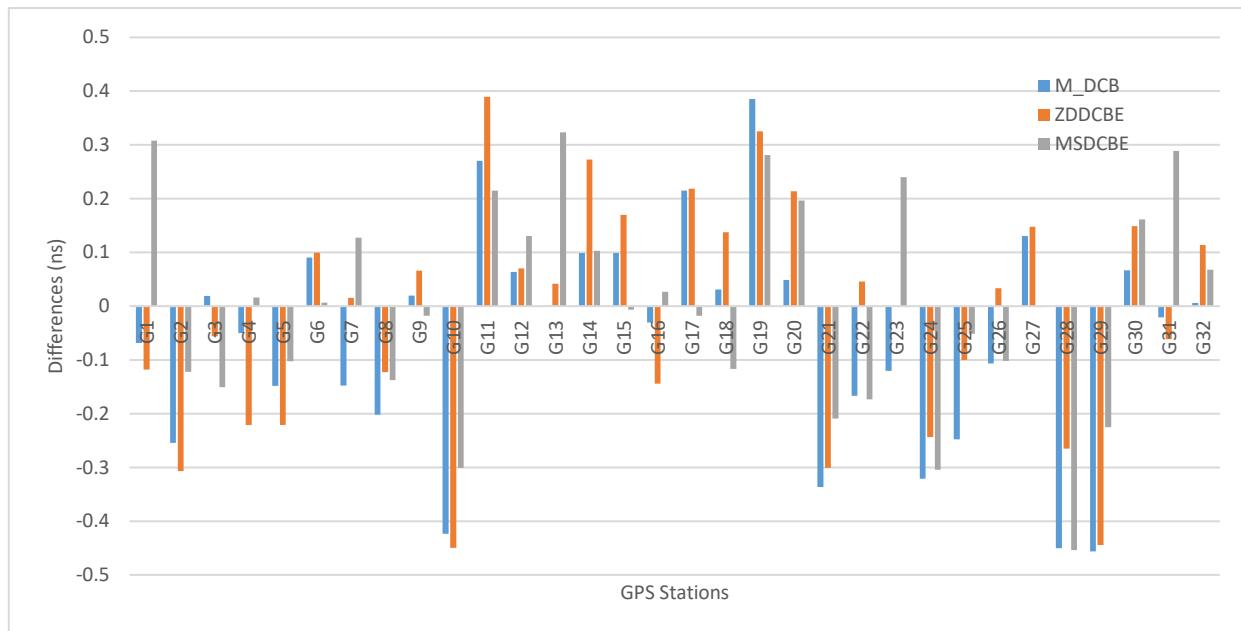
Figure 8 Mean difference between the satellites DCB values of IGS and the computed values by M_DCB, ZDDCBE and MSDCBE estimated from (1-5) Jan 2010

Conclusions

The current study proposes a new MATLAB code called MSDCBE able to calculate DCBs of GPS satellites and receivers. This code was compared with two other codes and evaluated using IAAC data and from all the above, we can conclude that:

1. The estimated DCBs results are affected by using weight function according to satellite elevation angle observations. In addition, results show a good agreement with IGS, CODE and JPL results than using multi station estimation DCB without weight function.

2. When using multi station DCB estimation, number of input stations influences in DCB results. However, it is recommended to enlarge the size of used network, but it needs high computer requirements and much more analysis time (only one station have more than 20,000 observation per a day).

3. The most effective factor in DCBs estimation is using multi station network instead of single station that appeared from results which improved from 1.1866 ns and 0.7982 ns maximum DCB mean differences for M_DCB and ZDDCBE single station analysis to 0.1477 ns for MSDCBE. So, using multi station network DCB estimation- if available- is strongly recommended.

References

Abid, M., Mousa, A., Rabah, M., El mewafi, M., and Awad, A.: Temporal and spatial variation of differential code biases: A case study of regional network in Egypt, Alexandria Engineering Journal, 55, 1507–1514, 2016.

Al-Fanek, O.: Ionospheric Imaging for Canadian Polar Regions, PhD thesis, Calgary, Alberta, 2013.

Arikan, F., Nayir, H., Sezen, U., Arikan, O.: Estimation of single station interfrequency receiver bias using GPS-TEC, Radio Sci. 43 (4). http://dx.doi.org/10.1029/2007rs003785, 2008.

248 Böhm, J., and Schuh, H.: Atmospheric Effects in Space Geodesy, Springer Atmospheric Sciences, eBook ISBN :978-3-642-
249   36932-2, 2013.

250 Elghazouly, A., Doma, M., Sedeek, A., Rabah, M., Hamama, M.: Validation of Global TEC Mapping Model Based on
251   Spherical Harmonic Expansion towards TEC Mapping over Egypt from a Regional GPS Network, American Journal of
252   Geographic Information System 2019, 8(2): 89-95 DOI: 10.5923/j.ajgis.20190802.04.

253 Feltens, J., and Schaer, S.: IGS Products for the Ionosphere, Proceedings of the 1998 IGS Analysis Center Workshop
254   Darmstadt, Germany,1998.

255 Ghilani, C., and Wolf, P.: Elementary surveying: an introduction to geomatics-13th ed, 2012.

256 Haines, G.: Spherical cap harmonic analysis, J Geophys Res Solid Earth 1985;90(B3):2583e91, 1985.

257 Hansen, A.: Tomographic Estimation of the Ionosphere Using GPS Sensors, PhD Thesis, Department of Electrical
258   Engineering, Stanford University, CA, 2002.

259 Hernández-Pajares, M., Juan, J., Sanz, J.: New approaches in global ionospheric determination using ground GPS data. Atmos
260   Solar Terr Phys 61:1237–1247, 1999.

261 Komjathy, A., Sparks, L., Wilson, BD., Mannucci, AJ.: Automated daily processing of more than 1000 ground-based GPS
262   receivers for studying intense ionospheric storms. Radio Sci 40:RS6006, doi:10.1029/2005RS003279,2005.

263 Jin, R., Jin, S., and Feng, G.: M_DCB: MATLAB code for estimating GPS satellite and receiver differential code biases, GPS
264   Solution 16:541–548, 2012.

265 Jin, S., Luo, O., and Park, P.: GPS observations of the ionospheric F2-layer behavior during the 20th November 2003
266   geomagnetic storm over South Korea, Journal of Geodesy, 82(12):883–892, 2008.

267 Leandro, R.: Precise Point Positioning with GPS: A New Approach for Positioning, Atmospheric Studies, and Signal Analysis,
268   Ph.D. dissertation, Department of Geodesy and Geomatics Engineering, Technical Report No. 267, University of New
269   Brunswick, Fredericton, New Brunswick, Canada, 232 pp, 2009.

270 Leick, A., Rapoport, L., and Tatarnikov, D.: GPS satellite surveying, Wiley, New York, 2015.

271 Li, Z., Yuan, Y., Wang, N., Hernandez-Pajares, M., and Huo, X.: SHPTS: towards a new method for generating precise global
272   ionospheric TEC map based on spherical harmonic and generalized trigonometric series functions, J Geodesy 89(4):331–
273   345, 2015.

274 Liu, Z., and Gao,Y.: Ionospheric TEC predictions over a local area GPS reference network, GPS Solut 8:23–29, 2004.

275 Luo, X.: GPS Stochastic Modelling: Signal Quality Measures and ARMA Processes, PhD thesis, the Karlsruhe Institute of
276   Technology, Karlsruhe, Germany, 2013.

277 Mannucci, AJ., Wilson, BD., Edwards, CD.: A new method for monitoring the Earth's ionospheric total electron content using
278   the GPS global network. In: Proceedings of ION GPS-93, the 6th international technical meeting of the satellite division
279   of The Institute of Navigation, Salt Lake City, UT, 22–24 September 1993, pp 1323–1332, 1993.

280 Mannucci, A., Wilson, B., Yuan, D., Ho, C., Lindqwister, U., and Runge, T.: Global mapping technique for GPS-derived
281   ionospheric total electron content measurements, RadioSci.33(3),565–582, 1998.

282 McCaffrey, A., Jayachandran, P., Themens, D., and Langley, R.: GPS receiver code bias estimation: A comparison of two
283   methods. Elsevier, Advances in Space Research 59 1984–1991, 2017.

284 Orús,R., Hernández-Pajares, M., Juan, J., and Sanz, J.: Improvement of global ionospheric VTEC maps by using kriging
285   interpolation technique, J.Atmos.Sol.Terr.Phys.67(16),1598–1609, 2005.

286 Ray, J., and Griffiths, J.: Overview of IGS products and analysis center modeling. Paper preseted at the IGS Analysis Center
287   Workshop 2008, Miami Beach, FL, 2–6 June,2008.

288 Schaer, S.: Mapping and predicting the earth's ionosphere using global positioning system, Ph.D. dissertation, Astronomy
289   Institute, University Bern, Switzerland, 205 pp, 1999.

290 Sedeek, A., Doma, M., Rabah, M., and Hamama, M.: Determination of zero difference GPS differential code biases for
291   satellites and prominent receiver types, Arab J Geosci, DOI 10.1007/s12517-017-2835-1, 2017.

292 Themens, D.R., Jayachandran, P.T., Langley, R.B., MacDougall, J.W., Nicolls, M.J.: Determining receiver biases in GPS-
293   derived total electron content in the auroral oval and polar cap region using ionosonde measurements, GPS Solut. 17 (3),
294   357–369. http://dx.doi.org/10.1007/s10291-012-0284-6, 2013.

295 Themens, D.R., Jayachandan, P.T., Langley, R.B.: The nature of GPS differential receiver bias variability: An examination in
296   the polar cap region, J. Geophys. Res.: Space Phys. 120 (9), 8155–8175. http:// dx.doi.org/10.1002/2015ja021639, 2015.

297 Zhang, B., Peter, J. G., Teunessen, Y., Hongxing, Z., and Min, L.: "Joint estimation of vertical total electron content (VTEC)
298   and satellite differential code biases (SDCBs) using low-cost receivers" J. Geod. 92: 401-413, 2018.

299